Improving the linearity of the Michelson interferometric angular measurement by a parameter compensation method

Pan Shi and E. Stijns

A parameter compensation method is developed to improve the linearity of the Michelson interferometric angular measurement. The formulas for the exact calculation of the parameters are presented; different cases are discussed. By introducing a weight function in the calculation, we can change the distribution of the linearity over the whole range of measurement. The theoretical analysis and the experimental results show that this method greatly improves the linearity of the measurement even for a large range of measurement.

Key words: Metrology, interferometry.

1. Introduction

Most methods of angular measurement based on a Michelson interferometer have the same principle: the rotation is transformed into an optical path difference (OPD); the measurement of the OPD (by measuring the shift of the interference fringes) gives, after calibration, the angle of rotation.[1–14] Figure 1 shows a possible setup.[15] Unfortunately, the transformation between the angle and the OPD is usually not linear. In fact the OPD is, in general, a sinusoidal function of the rotating angle; only for small angles (a few degrees) can the sine be approached by a linear function. Here we present a parameter compensation method (PCM) with which good linearity can be achieved even for large angles.

2. Principle

We calculated[15,16] that, for the one-prism setup shown in Fig. 1, the OPD as a function of rotating angle θ is

$$\Delta P = \left(\sqrt{2}a - 2x + 2y \tan\frac{\theta}{2}\right)\sin\theta - \sqrt{2}an(1 - \cos\alpha), \tag{1}$$

where a is the size of the right-angle prism, n is its refractive index, with $\alpha = \sin^{-1}(\sin\theta/n)$, and x and y are the position parameters of the axis of rotation of the rotating table as shown in Fig. 1.

We write this formula as

$$\Delta P = \Delta P_0 + \Delta P_1 - \Delta P_2, \tag{2}$$

where

$$\Delta P_0 = (\sqrt{2}a - 2x)\sin\theta,$$

$$\Delta P_1 = 2y \tan\frac{\theta}{2}\sin\theta,$$

$$\Delta P_2 = \sqrt{2}an(1 - \cos\alpha).$$

ΔP_0 is a sinusoidal function of θ; it is also the main part of ΔP. ΔP_1 and ΔP_2 are much smaller than ΔP_0; they are the additional OPD caused by position parameter y and by the rotation of the prism itself. In fact the OPD inside the prism is also a function of the rotating angle.

For the balanced two-prism setup shown in Fig. 2, the OPD as a function of rotating angle θ is

$$\Delta P = 2(\sqrt{2}a + 2d)\sin\theta, \tag{3}$$

where $2d$ is the distance between the two right-angle prisms shown in Fig. 2. It can also be simplified to

$$\Delta P = 4r\sin\theta, \tag{4}$$

where r is the radius of the rotation of the two prisms.

When this research was performed the authors were with Algemene Natuurkunde, Faculteit Toegepaste Wetenschappen, Vrije Universiteit Brussel, Pleinlaan 2, B-1050 Brussels, Belgium. P. Shi is now with the Department of Physics, Dalian University of Technology, 116024 Dalian, China.

Received 11 December 1991.
0003-6935/93/010044-08$05.00/0.

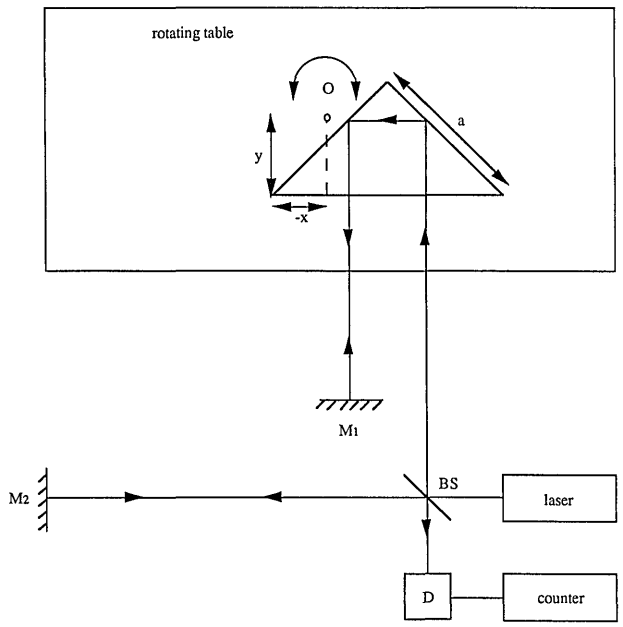

Fig. 1. Michelson interferometric angular measurement setup with one prism: M1, M2, mirrors; D, photodetector; BS, beam splitter.

The symmetry makes the formula simple: the additional OPD's of the two prisms cancel each other. Moreover, the position of the center of rotation is not important, so x and y do not appear in the formula.

In order to have a clear idea of the deviations from linearity we define a degree of nonlinearity L_n as

$$L_n = \frac{N_\theta - \theta e}{\theta e}, \tag{5}$$

where N_θ is the number of fringes that we get for turning the rotating table over $\theta°$ and e is the equivalence of the angular measurement, i.e., the number of fringes for 1°.

The linearity of the two-prism setup is the same as the linearity of a standard sine function. L_n's of 1°, 5°, 10°, and 20° are 0, 0.0012, 0.002, and 0.02, respectively. The linearity of the one-prism setup is rather complicated; it depends on x, y, θ, and n. In what follows we concentrate on this one-prism setup. Analysis of the L_n shows that, if n is constant, for some values of x and y L_n is better than the L_n of a standard sine function. The reason is the following: When we choose certain values of x and y for a small angle θ, ΔP_1 and ΔP_2 cancel each other; consequently the linearity of ΔP depends only on ΔP_0, which is good. When the angle θ increases, ΔP_1 and ΔP_2 do not totally cancel each other any more, but they leave a small quantity that compensates for the nonlinearity of the sine term of ΔP_0; so one obtains good linearity for ΔP. This is the basic idea of the PCM. Theoretical analysis shows that it is possible to choose the position parameters x and y to realize the PCM.

In Michelson interferometric angular measurement, when the rotating table is turned over an angle θ the OPD is ΔP; the number of interference fringes passing the detector is N, and we have

$$N = \frac{2\Delta P}{\lambda}. \tag{6}$$

(N is also the number of pulses that we get from the counter if we do not use a fringe divider.) For the measurement with ideal linearity, we should have

$$N_{\text{ideal}} = \theta e \tag{7}$$

or

$$\Delta P_{\text{ideal}} = \frac{\theta e \lambda}{2}. \tag{8}$$

The difference between the real number of fringes in the measurement and the ideal number of fringes that we hope to get is called the error (indeed it is the deviation from linearity):

$$\text{error} = N - N_{\text{ideal}} = \frac{2\Delta P}{\lambda} - \theta e. \tag{9}$$

The PCM consists of finding a pair of parameters x and y with which N approaches N_{ideal} or, in other words, making the error minimum for the whole range of measurement. The principle of the PCM is explained in Fig. 3. If

$$N_1 - N_2 = N_{\text{ideal}} - N_0, \tag{10}$$

then

$$N = N_0 + N_1 - N_2 = N_{\text{ideal}}. \tag{11}$$

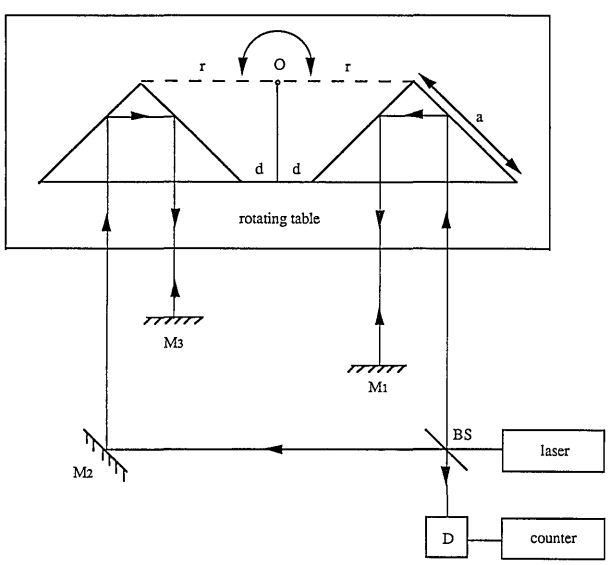

Fig. 2. Balanced Michelson interferometric angular measurement setup with two prisms: M1–M3, mirrors; D, photodetector; BS, beam splitter.

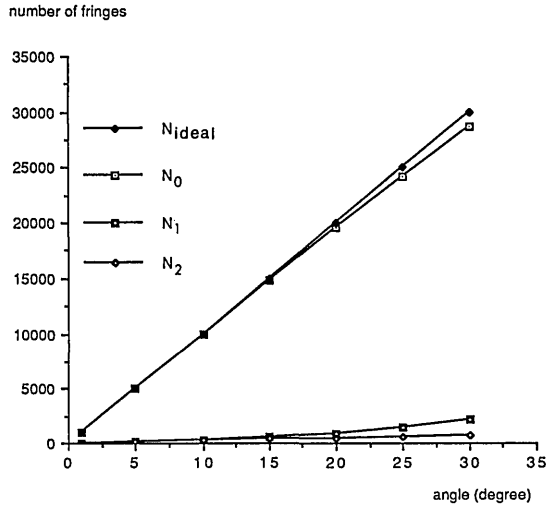

Fig. 3. Principle of the PCM.

3. Calculation of Position Parameters x and y

In this section the PCM is applied to the single-prism setup of Fig. 1. In order to find parameters x and y, we rewrite Eq. (1) as

$$\Delta P_i = \left(\sqrt{2}a + 2x + 2y \tan\frac{i}{2}\right)\sin i - \sqrt{2}a[n - (n^2 - \sin^2 i)^{1/2}], \quad i = 1, 2, \ldots \theta°, \tag{12}$$

where x has been replaced by $-x$ so it will conform with Fig. 1. Other possibilities are discussed in Section 4.

$$\text{Error}_i = N_i - N_{\text{ideal}} = \frac{2\Delta P_i}{\lambda} - ie, \quad i = 1, 2, \ldots \theta°. \tag{13}$$

For this set of linear equations, it is not possible to determine one pair of x, y that makes $\text{error}_i = 0$ for all $i = 1, 2, \ldots \theta°$. We can use only the optimization method to find a pair of x and y that makes

$$\sum_{i=1}^{\theta} \text{error}_i^2 \text{ minimum},$$

i.e.,

$$\min \sum_{i=1}^{\theta} (2\Delta P_i/\lambda - ie)^2 = \min \sum_{i=1}^{\theta} \frac{4}{\lambda^2}\left\{2x \sin i + 2y \tan\frac{i}{2}\sin i + \sqrt{2}a \sin i - \sqrt{2}a[n - (n^2 - \sin^2 i)^{1/2}] - \frac{\lambda ie}{2}\right\}^2 = \min \sum_{i=1}^{\theta} \frac{4}{\lambda^2}(A_i x + B_i y + C_i)^2, \tag{14}$$

where

$$A_i = 2 \sin i, \tag{15}$$

$$B_i = 2 \tan\frac{i}{2}\sin i, \tag{16}$$

$$C_i = \sqrt{2}a \sin i - \sqrt{2}a[n - (n^2 - \sin^2 i)^{1/2}] - \frac{\lambda ie}{2}, \quad i = 1, 2, \ldots \theta°. \tag{17}$$

For the x and y that make

$$\sum_{i=1}^{\theta} \text{error}_i^2 \text{ minimum},$$

we have

$$\frac{\partial}{\partial x}\sum_{i=1}^{\theta} \text{error}_i^2 = 0, \tag{18}$$

$$\frac{\partial}{\partial y}\sum_{i=1}^{\theta} \text{error}_i^2 = 0, \tag{19}$$

i.e.,

$$\frac{\partial}{\partial x}\sum_{i=1}^{\theta} (A_i x + B_i y + C_i)^2 = 0, \tag{20}$$

$$\frac{\partial}{\partial y}\sum_{i=1}^{\theta} (A_i x + B_i y + C_i)^2 = 0. \tag{21}$$

This leads to two coupled linear equations:

$$x\sum_{i=1}^{\theta} A_i^2 + y\sum_{i=1}^{\theta} A_i B_i = -\sum_{i=1}^{\theta} A_i C_i, \tag{22}$$

$$x\sum_{i=1}^{\theta} A_i B_i + y\sum_{i=1}^{\theta} B_i^2 = -\sum_{i=1}^{\theta} B_i C_i. \tag{23}$$

Solving these coupled equations gives

$$x = \frac{\sum_{i=1}^{\theta} A_i B_i \sum_{i=1}^{\theta} B_i C_i - \sum_{i=1}^{\theta} A_i C_i \sum_{i=1}^{\theta} B_i^2}{\sum_{i=1}^{\theta} A_i^2 \sum_{i=1}^{\theta} B_i^2 - \left(\sum_{i=1}^{\theta} A_i B_i\right)^2}, \tag{24}$$

$$y = \frac{\sum_{i=1}^{\theta} A_i B_i \sum_{i=1}^{\theta} A_i C_i - \sum_{i=1}^{\theta} A_i^2 \sum_{i=1}^{\theta} B_i C_i}{\sum_{i=1}^{\theta} A_i^2 \sum_{i=1}^{\theta} B_i^2 - \left(\sum_{i=1}^{\theta} A_i B_i\right)^2}. \tag{25}$$

For $a = 30$ mm, $n = 1.517$, $e = 10^3$, we calculated the parameters x and y, the number of fringes, the error, and the degree of nonlinearity. The results are

Table 1. Comparison of Fringes, Error, and Nonlinearity between the PCM and the Sine Function for a Measuring Range of 5°

	PCM[a]			Sinusoidal Function Compared with the PCM		
Angle θ (deg)	Fringes $N_\theta = 2\Delta P/\lambda$	Error $\delta = N_\theta - \theta e$	Nonlinearity $L_n = \delta/(\theta e)$ (1/10,000)	Nonlinearity $L_n = \delta/(\theta e)$ (1/10,000)	Error $\delta = N_\theta - \theta e$	Fringes $N_\theta = e \sin\theta/\sin 1$
1	1000	0	0	0	0	1000
2	2000	0	0	0	0	2000
3	3000	0	0	−3.33	−1	2999
4	4000	0	0	−7.5	−3	3997
5	5000	0	0	−12	−6	4994

[a] $a = 30$ mm, $n = 1.517$, $e = 1000$ with $x = -12.154$ mm, $y = 14.337$ mm.

Table 2. Comparison of Fringes, Error, and Nonlinearity between the PCM and the Sine Function for a Measuring Range of 10°

	PCM[a]			Sinusoidal Function Compared with the PCM		
Angle θ (deg)	Fringes $N_\theta = 2\Delta P/\lambda$	Error $\delta = N_\theta - \theta e$	Nonlinearity $L_n = \delta/(\theta e)$ (1/10,000)	Nonlinearity $L_n = \delta/(\theta e)$ (1/10,000)	Error $\delta = N_\theta - \theta e$	Fringes $N_\theta = e \sin\theta/\sin 1$
1	999	−1	−10	0	0	1000
2	1999	−1	−5	0	0	2000
3	2999	−1	−3	−3.33	−1	2999
4	4000	0	0	−7.5	−3	3997
5	5001	1	2	−12	−6	4994
6	6001	1	1.66	−18.3	−11	5989
7	7002	2	2.86	−24.3	−17	6983
8	8002	2	2.5	−32.5	−26	7974
9	9001	1	1.1	−41.1	−37	8963
10	9999	−1	−1	−50	−50	9950

[a] $a = 30$ mm, $n = 1.517$, $e = 1000$ with $x = -12.165$ mm, $y = 14.623$ mm.

Table 3. Comparison of Fringes, Error, and Nonlinearity between the PCM and the Sine Function for a Measuring Range of 20°

	PCM[a]			Sinusoidal Function Compared with the PCM		
Angle θ (deg)	Fringes $N_\theta = 2\Delta P/\lambda$	Error $\delta = N_\theta - \theta e$	Nonlinearity $L_n = \delta/(\theta e)$ (1/10,000)	Nonlinearity $L_n = \delta/(\theta e)$ (1/10,000)	Error $\delta = N_\theta - \theta e$	Fringes $N_\theta = e \sin\theta/\sin 1$
1	995	−5	−50	0	0	1000
2	1992	−8	−40	0	0	2000
3	2991	−9	−30	−3.33	−1	2999
4	3991	−9	−22.5	−7.5	−3	3997
5	4992	−8	−16	−12	−6	4994
6	5993	−7	−11.6	−18.3	−11	5989
7	6995	−5	−7.14	−24.3	−17	6983
8	7998	−2	−2.5	−32.5	−26	7974
9	9000	0	0	−41.1	−37	8963
10	10,002	2	2	−50	−50	9950
11	11,004	4	3.64	−60.91	−67	10,933
12	12,006	6	5	−72.5	−87	11,913
13	13,007	7	5.38	−85.38	−111	12,889
14	14,007	7	5	−98.57	−138	13,862
15	15,007	7	4.67	−113.33	−170	14,830
16	16,005	5	3.13	−128.75	−206	15,794
17	17,003	3	1.76	−145.29	−247	16,753
18	18,000	0	0	−163.33	−294	17,706
19	18,995	−5	−2.63	−181.58	−345	18,655
20	19,989	−11	−5.5	−201.5	−403	19,597

[a] $a = 30$ mm, $n = 1.517$, $e = 1000$ with $x = -12.200$ mm, $y = 15.059$ mm.

shown in Tables 1, 2, and 3 for $\theta_{max} = 5°$, 10°, and 20°, respectively. We use the integral for the number of fringes and calculate x, y to an accuracy of 10^{-3} mm. As a comparison with the PCM we also list in the same tables the number of fringes, the error, and the degree of nonlinearity for the pure sine function.

Figures 4–6 show the comparison of the error between the PCM and the sine function. It is evident that, when the PCM is used, the linearity of the measurement can be greatly improved even for a large range of measurements.

In the calculation we can moreover introduce the weight of the error; in this case

$$\text{error}_i = w_i(N_i - N_{\text{ideal}}) = w_i\left(\frac{2\Delta P_i}{\lambda} - ie\right), \quad i = 1, 2, \ldots \theta°. \quad (26)$$

After the same calculation we obtain

$$x = \frac{\sum_{i=1}^{\theta} w_i^2 A_i B_i \sum_{i=1}^{\theta} w_i^2 B_i C_i - \sum_{i=1}^{\theta} w_i^2 A_i C_i \sum_{i=1}^{\theta} w_i^2 B_i^2}{\sum_{i=1}^{\theta} w_i^2 A_i^2 \sum_{i=1}^{\theta} w_i^2 B_i^2 - \left(\sum_{i=1}^{\theta} w_i^2 A_i B_i\right)^2}, \quad (27)$$

$$y = \frac{\sum_{i=1}^{\theta} w_i^2 A_i B_i \sum_{i=1}^{\theta} w_i^2 A_i C_i - \sum_{i=1}^{\theta} w_i^2 A_i^2 \sum_{i=1}^{\theta} w_i^2 B_i C_i}{\sum_{i=1}^{\theta} w_i^2 A_i^2 \sum_{i=1}^{\theta} w_i^2 B_i^2 - \left(\sum_{i=1}^{\theta} w_i^2 A_i B_i\right)^2}. \quad (28)$$

We used

$$w_i = (\theta - i + 1) \Big/ \sum_{i=1}^{\theta} i$$

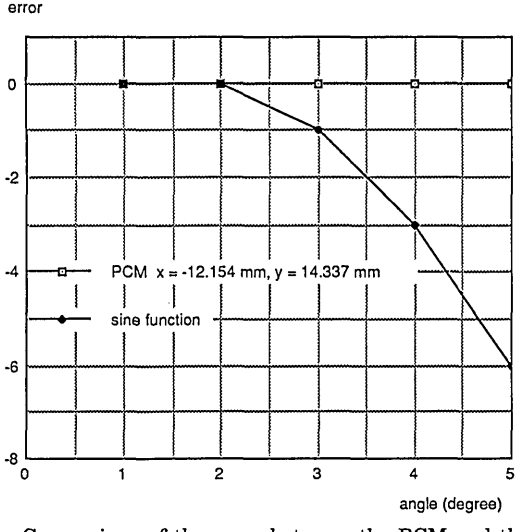

Fig. 4. Comparison of the error between the PCM and the sine function for a measuring range of 5°.

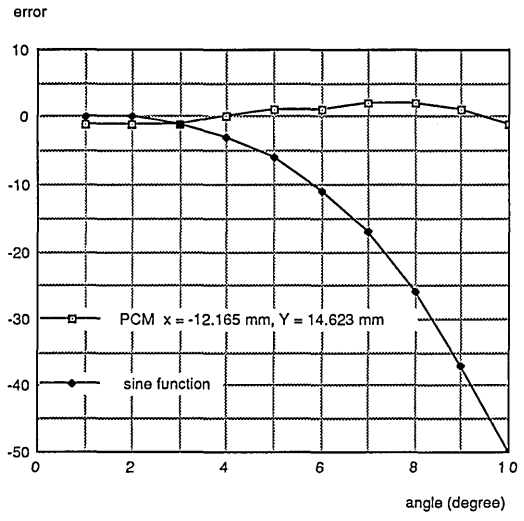

Fig. 5. Comparison of the error between the PCM and the sine function for a measuring range of 10°.

to calculate x and y. We chose this expression because it seems to be the simplest expression that gives a satisfactory correction of the nonlinearity. Table 4 shows the results of the nonlinearities, along with the values of the PCM of Table 3 for comparison.

In Table 4 the linearity for small angles is improved, but this improvement is at the expense of linearity for large angles because, for

$$w_i = (\theta - i + 1) \Big/ \sum_{i=1}^{\theta} i,$$

the weight is greater for small angles than for large ones. It is possible to use various w_i to change the distribution of the linearity in the whole range of measurements.

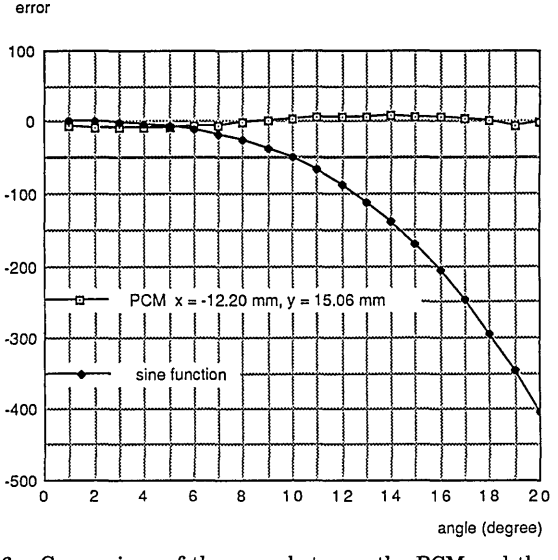

Fig. 6. Comparison of the error between the PCM and the sine function for a measuring range of 20°.

Table 4. Comparison of Fringes, Error, and Nonlinearity between the Two PCM's Using $w_i = 1$ and $w_i = (\theta - i + 1)/\Sigma i$

Angle θ (deg)	First PCM[a] Fringes $N_\theta = 2\Delta P/\lambda$	First PCM[a] Error $\delta = N_\theta - \theta e$	First PCM[a] Nonlinearity $L_n = \delta/(\theta e)$ (1/10,000)	Second PCM[b] Nonlinearity $L_n = \delta/(\theta e)$ (1/10,000)	Second PCM[b] Error $\delta = N_\theta - \theta e$	Second PCM[b] Fringes $N_\theta = e \sin\theta/\sin 1$
1	995	−5	−50	−30	−3	997
2	1992	−8	−40	−20	−4	1996
3	2991	−9	−30	−13.33	−4	2996
4	3991	−9	−22.5	−10	−4	3996
5	4992	−8	−16	−4	−2	4998
6	5993	−7	−11.6	−1.67	−1	5999
7	6995	−5	−7.14	1.43	1	7001
8	7998	−2	−2.5	3.75	3	8003
9	9000	0	0	4.44	4	9004
10	10,002	2	2	5	5	10,005
11	11,004	4	3.64	4.55	5	11,005
12	12,006	6	5	4.17	5	12,005
13	13,007	7	5.38	2.31	3	13,003
14	14,007	7	5	0.71	1	14,001
15	15,007	7	4.67	−2	−3	14,997
16	16,005	5	3.13	−5	−8	15,992
17	17,003	3	1.76	−8.82	−15	16,985
18	18,000	0	0	−12.22	−22	17,978
19	18,995	−5	−2.63	−16.8	−32	18,968
20	19,989	−11	−5.5	−21	−42	19,958

[a] $a = 30$ mm, $n = 1.517$, $e = 1000$, $W_i = 1$ with $x = -12.200$ mm, $y = 15.059$ mm.
[b] $a = 30$ mm, $n = 1.517$, $e = 1000$, $W_i = (\theta - i + 1)/\Sigma i$, with $x = -12.181$ mm, $y = 14.868$ mm.

4. Use of the Parameter Compensation Method in Different Cases of Rotation

There are different cases of rotation depending on the position of O (the center of rotation) and the direction of rotation. The four different positions of O are located by the two position parameters $\pm x$ and $\pm y$ (see Fig. 7); the two directions of rotation are indicated by $\pm\theta$ (see Fig. 8).

By direct calculation it is not difficult to show that, for the center of rotation in $O_1(-x, y)$ and $O_2(x, y)$, the direction of rotation is positive (i.e., the direction of rotation that causes the OPD increase) and the OPD after we rotate over $+\theta$ is

$$\Delta p = \left(\sqrt{2}a \pm 2x + 2y \tan\frac{\theta}{2}\right)\sin\theta - \sqrt{2}a[n - (n^2 - \sin^2\theta)^{1/2}], \quad (29)$$

where x has a positive sign for $O_2(x, y)$ and x has a negative sign for $O_1(-x, y)$. This formula can be written as

$$\Delta p = \Delta p_0 + \Delta p_1 - \Delta p_2, \quad (30)$$

where

$$\Delta p_0 = (\sqrt{2}a \pm 2x)\sin\theta, \quad (31)$$

$$\Delta p_1 = 2y \tan\frac{\theta}{2}\sin\theta, \quad (32)$$

$$\Delta p_2 = \sqrt{2}a[n - (n^2 - \sin^2\theta)^{1/2}]. \quad (33)$$

For $O_1(-x, y)$, $O_2(x, y)$, and $-\theta$, after calculations we obtain

$$\Delta p = \Delta p_0 - \Delta p_1 + \Delta p_2. \quad (34)$$

For $O_3(x, -y)$, $O_4(-x, -y)$, and $+\theta$, we have

$$\Delta p = \Delta p_0 - \Delta p_1 - \Delta p_2. \quad (35)$$

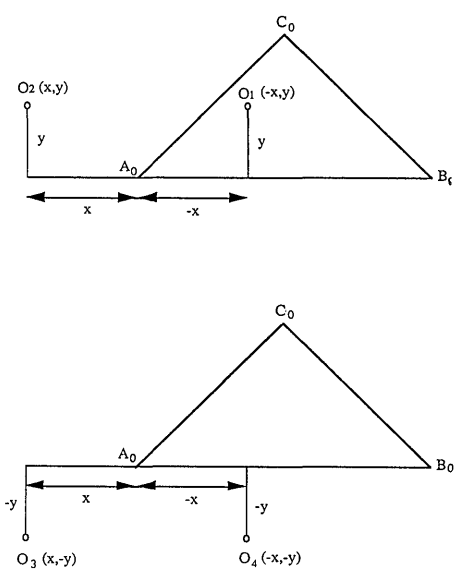

Fig. 7. Center of rotation in four different positions of O_1, O_2, O_3, and O_4.

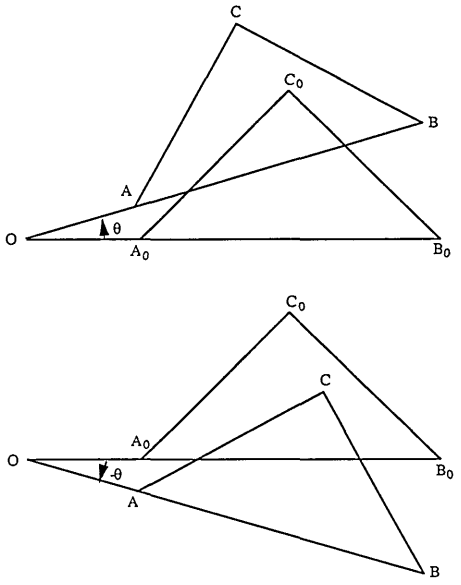

Fig. 8. Rotation in two different directions of $+\theta$ and $-\theta$.

For $O_3(x, -y)$, $O_4(-x, -y)$, and $-\theta$, we have

$$\Delta p = \Delta p_0 + \Delta p_1 + \Delta p_2. \tag{36}$$

We can write a uniform formula to cover all the above cases of rotation:

$$\Delta p = \left(\sqrt{2}a + 2x + 2y \tan\frac{\theta}{2}\right)\sin\theta - \sqrt{2}a[n - (n^2 - \sin^2\theta)^{1/2}]. \tag{37}$$

When we use the values of x, y, and θ together with their signs, we get a special case of rotation for each.

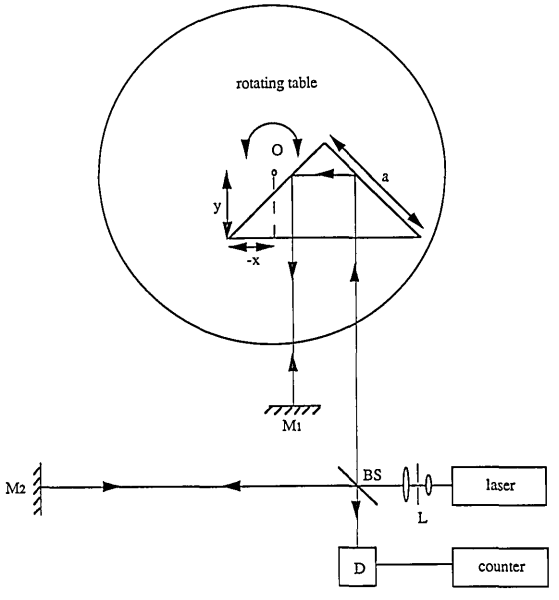

Fig. 9. Experimental setup that was used to check the linearity of the PCM: M1, M2, mirrors; D, photodetector; BS, beam splitter; L, lens.

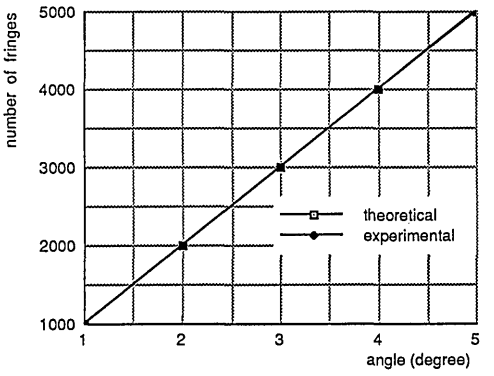

Fig. 10. Comparison of the experimental results and the theoretical line of $N_{ideal} = \theta e$.

It is evident that, when x has a positive sign, in other words when the center of rotation is in position O_2 or O_3, the sensibility increases: indeed, for the same angle of rotation, Δp_0 is greater for positions O_2 and O_3 than for positions O_1 and O_2. The PCM can be used in the following cases:

(A) $+y, +\theta$:

$$\Delta p = \Delta p_0 + \Delta p_1 - \Delta p_2,$$

for which compensation is made by $\Delta p_1 - \Delta p_2$;

(B) $+y, -\theta$:

$$\Delta p = \Delta p_0 - \Delta p_1 + \Delta p_2,$$

for which compensation is made by $\Delta p_2 - \Delta p_1$;

(C) $-y, -\theta$:

$$\Delta p = \Delta p_0 + \Delta p_1 + \Delta p_2,$$

for which compensation is made by $\Delta p_1 + \Delta p_2$.

5. Experiment and Results

We built the experimental setup of Fig. 9 to check the linearity of the PCM. Light from the He–Ne laser light source was divided into two subbeams: one is reflected by mirror 2 (M2) and the other passes the prism and is backreflected by mirror 1 (M1). The photodiode detects the interference pattern formed by the recombined two subbeams; after amplification the signals were counted by the counter. To check the linearity of the PCM, we set the center of rotation at $x = -12.15$ mm, $y = 14.34$ mm, as shown in Fig. 9. These results are shown in Fig. 10, which should be compared with the uncompensated Fig. 3. The experimental results coincide with the theoretical line and have good linearity.

6. Conclusion

The parameter compensation method is a simple method to improve the linearity of Michelson interfer-

ometric angular measurements for a single-prism setup as shown in Fig. 1. The position parameters can be calculated exactly; when the rotating center is set at this position, good linearity can be achieved. With the use of weight functions, we can change the distribution of the linearity in the whole range of measurements.

References

1. E. R. Peck, "A new principle in interferometer design," J. Opt. Soc. Am. **38,** 66 (1948).
2. E. R. Peck, "Theory of the corner-cube interferometer," J. Opt. Soc. Am. **38,** 1015–1024 (1948).
3. E. R. Peck, "Uncompensated corner-reflector interferometer," J. Opt. Soc. Am. **47,** 250–252 (1957).
4. R. A. Woodson, "Differential Woodson interferometer," J. Opt. Soc. Am. **51,** 1467(A) (1961).
5. R. A. Woodson, "Extended-range Gonimet angle interferometer," J. Opt. Soc. Am. **52,** 1315(A) (1962).
6. J. Rohlin, "An interferometer for precision angle measurements," Appl. Opt. **2,** 762–763 (1963).
7. M. V. R. K. Murty, "Modification of Michelson interferometer using only one cube-corner prism," J. Opt. Soc. Am. **50,** 83–84 (1960).
8. J. G. Marzolf, "Angle measuring interferometer," Rev. Sci. Instrum. **35,** 1212–1215 (1964).
9. D. Malacara and O. Harris, "Interferometric measurement of angles," Appl. Opt. **9,** 1630–1633 (1970).
10. H. M. Bird, "A computer controlled interferometer system for precision relative angle measurements," Rev. Sci. Instrum. **42,** 1513–1520 (1971).
11. G. D. Chapman, "Beam pathlength multiplication," Appl. Opt. **13,** 679–683 (1974).
12. G. D. Chapman, "Interferometric angular measurement," Appl. Opt. **13,** 1646–1651 (1974).
13. E. Debler, "Winkelinterferometer mit einem Messbereich von 95°," Feinwerktech. & Messtech. **85,** 166–171 (1977).
14. P. Shi and E. Stijns, "Highly sensitive angular measurement with Michelson interferometer," Ind. Metrol. **1,** 69–74 (1990).
15. P. Shi and E. Stijns, "New optical method for measuring small-angle rotations," Appl. Opt. **27,** 4342–4344 (1988).
16. P. Shi and E. Stijns, "A new optical method for measuring small angle rotations," in *Proceedings of the International Conference on Lasers '87* (STS, McLean, Va., 1987) pp. 1609–1072.